water

MDPI

Article

A Real-Time Prediction Approach to Deep Soil Moisture Combining GNSS-R Data and a Water Movement Model in Unsaturated Soil

Xiaotian Luo [1,2], Cong Yin [2,3], Yueqiang Sun [2,3], Weihua Bai [2,3], Wei Li [2,3] and Hongqing Song [1,2,*]

[1] School of Civil and Resource Engineering, University of Science and Technology Beijing, Beijing 100083, China; d202210002@xs.ustb.edu.cn
[2] Joint Lab for Application of GNSS Atmospheric Remote Sensing Data, Beijing 100083, China
[3] National Space Science Center, Chinese Academy of Sciences (NSSC/CAS), Beijing 100190, China
* Correspondence: songhongqing@ustb.edu.cn

Abstract: Deep soil moisture data have wide applications in fields such as engineering construction and agricultural production. Therefore, achieving the real-time monitoring of deep soil moisture is of significant importance. Current soil monitoring methods face challenges in conducting the large-scale, real-time monitoring of deep soil moisture. This paper innovatively proposes a real-time prediction approach to deep soil moisture combining GNSS-R data and a water movement model in unsaturated soil. This approach, built upon surface soil moisture data retrieved from GNSS-R signal inversion, integrates soil–water characteristics and soil moisture values at a depth of 1 m. By employing a deep soil moisture content prediction model, it provides predictions of soil moisture at depths from 0 to 1 m, thus realizing the large-scale, real-time dynamic monitoring of deep soil moisture. The proposed approach was validated in a study area in Goodwell, Texas County, Oklahoma, USA. Predicted values of soil moisture at a randomly selected location in the study area at depths of 0.1 m, 0.2 m, 0.5 m, and 1 m were compared with ground truth values for the period from 25 October to 19 November 2023. The results indicated that the relative error (δ) was controlled within the range of $\pm$14%. The mean square error (MSE) ranged from 2.90×10^{-5} to 1.88×10^{-4}, and the coefficient of determination (R^2) ranged from 82.45% to 89.88%, indicating an overall high level of fitting between the predicted values and ground truth data. This validates the feasibility of the proposed approach, which has the potential to play a crucial role in agricultural production, geological disaster management, engineering construction, and heritage site preservation.

Keywords: deep soil moisture; soil–water characteristics; mathematical model; prediction; GNSS-R

check for updates

Citation: Luo, X.; Yin, C.; Sun, Y.; Bai, W.; Li, W.; Song, H. A Real-Time Prediction Approach to Deep Soil Moisture Combining GNSS-R Data and a Water Movement Model in Unsaturated Soil. *Water* **2024**, *16*, 979. https://doi.org/10.3390/w16070979

Academic Editors: María del Carmen Cabrera Santana, Albert Casas Ponsati and Alex Sendros

Received: 17 February 2024
Revised: 26 March 2024
Accepted: 26 March 2024
Published: 28 March 2024

1. Introduction

Water in soil exists in various forms, including structural water, bound water, free water, solid-state water, and gaseous water. Investigating the quantity of water in soil is of paramount importance [1,2]. The amount of water in soil is typically expressed as moisture content, which fundamentally represents the ratio of water, excluding structural water, to the mass or volume of the solid or soil body. This can be expressed in two primary methods: mass moisture content and volumetric moisture content. Buckingham and Gardner conducted initial research on the amount of water with respect to the energy level with which water is held in the soil, and the relationship is known as the soil water characteristic curve (SWCC) [3,4]. SWCC is a relationship between the moisture content in the soil and soil suction (soil moisture potential), and it is unique for each soil type. SWCC is used to predict soil moisture storage and field capacity and to understand the drying and wetting characteristics of the soil and its pore structure [5,6]. The water movement equation in unsaturated soil is a mathematical model describing the process of water movement within soil, which holds significant importance in understanding soil moisture distribution, hydrological cycles, and agricultural irrigation practices. Water movement in soil is typically influenced by soil properties, initial moisture conditions, boundary conditions, and environmental factors. In the early 20th century, Richards proposed the renowned Richards equation, which has been widely employed to describe water movement in unsaturated soil. This equation, grounded on Darcy's law and the principle of mass conservation, incorporates factors such as soil moisture, soil water potential, and hydraulic conductivity, and it has been extensively utilized to investigate various scenarios of soil water movement [7]. As research progressed, scholars recognized limitations in the Richards equation when describing certain situations, such as nonlinearity and a lack of physical interpretability. Consequently, to address these issues, several improved models have been proposed, including the Brooks–Corey model, the Van Genuchten model, and others [8,9]. These models take into account factors such as soil pore structure and capillary pressure curves, providing a more accurate description of the soil moisture movement process. In determining soil engineering properties, controlling the quality of compacted soil construction, monitoring and forecasting geological hazards, managing agricultural production with precision, and preserving cultural relics, it is essential to conduct the testing and monitoring of soil moisture conditions [10,11]. Therefore, achieving the real-time monitoring of deep soil moisture holds significant importance.

Surface soil moisture can be retrieved through GNSS-R signals, meeting the demand for all-weather autonomous monitoring. GNSS, which stands for Global Navigation Satellite System, primarily includes the United States GPS system, China's BDS system, Russia's GLONASS system, and the European Union's GALILEO system [12]. These navigation satellites not only provide navigation positioning and timing information to users in real-time but also offer L-band microwave signals suitable for remote sensing detection characterized by global coverage, strong penetration, and a high temporal resolution [13]. Retrieving soil moisture data from GNSS-R signals involves capturing both direct and reflected satellite signals, analyzing the time delay or power changes of the surface-reflected signals, and deducing relevant parameters reflecting surface features based on the geometric relationships among GNSS satellites, ground receivers, reflection points, and the variations in reflection signal characteristics and surface soil properties. The technology for retrieving surface soil moisture data through GNSS-R signals has become relatively mature. In 2002, the University of Colorado and others, under the leadership of NASA, conducted a series of soil moisture retrieval experiments, and experimental data validated the accuracy of the monitoring results [14]. The Starlab Institute in Spain has designed a soil moisture detection device based on L-band GNSS signal observations. This device analyzes the GNSS signals after interference to obtain relevant information about soil moisture [15]. Utilizing the Advanced Integrated Equation Model (AIEM), a method for soil moisture monitoring was derived, and the accuracy of the GNSS-R soil moisture monitoring model was validated based on existing experimental data [16].

Current soil monitoring methods face challenges in achieving the large-scale, real-time monitoring of deep soil moisture. Various methods are available for soil moisture monitoring, including the drying–weighing method, Time Domain Reflectometry (TDR), Ground Penetrating Radar (GPR), the soil resistance method, and the capacitance method for single-point or small-scale soil moisture monitoring. Remote sensing technology is commonly used for spatial and temporal distribution and changes in soil moisture over large areas [17–41]. However, several issues persist in real-time soil moisture monitoring. For instance, the applicability and accuracy of testing methods are often influenced and constrained due to soil characteristics. Furthermore, instruments and sensors commonly suffer from issues such as a large size, high energy consumption, and a high cost, resulting in high real-time monitoring expenses [17–19]. The L-band signals carried by Global Navigation Satellite Systems (GNSSs) are highly sensitive to soil moisture, making them particularly suitable for monitoring soil moisture variations [42]. By utilizing signal power or delay as attributes and actual soil moisture values as labels, inversion models based on navigation signals can be established through the combination of empirical dielectric constant models, Support Vector Machines (SVMs), Random Forest algorithms, and neural network methods such as BP and Deep Belief Networks [43–45]. Therefore, the introduction of soil moisture data retrieved from GNSS-R signals largely overcomes the limitations of traditional soil moisture measurement methods in terms of small effective measurement area and a lack of representativeness, meeting the demand for all-weather autonomous monitoring. However, the penetration depth of GNSSs' L-band signals is limited to only 10 cm. As a result, soil moisture data within 10 cm depth can be retrieved through GNSS-R signal inversion, and soil moisture data within 5 cm depth can be more accurately inverted through GNSS-R signals. In summary, current soil monitoring methods face challenges in achieving the large-scale, real-time monitoring of deep soil moisture. However, deep soil moisture data are crucial in agriculture, geological hazard monitoring, engineering construction, and site preservation.

Therefore, by integrating soil–water characteristics and soil moisture at a depth of 1 m with surface soil moisture data retrieved from GNSS-R signal inversion, deep soil moisture prediction models can be developed. These models enable the prediction of soil moisture values in the 0–1 m depth range, facilitating the large-scale, real-time dynamic monitoring of deep soil moisture.

This paper addresses the current challenge of the inability of existing soil moisture monitoring methods to achieve the large-scale, real-time dynamic monitoring of deep soil moisture. It innovatively proposes a real-time prediction approach to deep soil moisture combining GNSS-R data and water movement model in unsaturated soil. This approach, relying on soil moisture data retrieved from GNSS-R signal inversion, largely overcomes the limitations of traditional soil moisture measurement methods, such as small effective measurement areas and a lack of representativeness, thereby meeting the demand for all-weather autonomous monitoring. By integrating soil–water characteristics and soil moisture values at a depth of 1 m with surface soil moisture data retrieved from GNSS-R signal inversion, the approach can predict soil moisture values in the 0–1 m depth range. This approach overcomes the limitation of GNSS-R signal inversion, which is restricted to the soil surface. The proposed method realizes the large-scale, real-time dynamic monitoring of deep soil moisture and is expected to play a crucial role in agriculture, geological hazard monitoring, engineering construction, and site preservation.

2. Methodology

2.1. Method Design

The core of this real-time prediction approach to deep soil moisture combining GNSS-R data and a water movement model in unsaturated soil lies in the prediction model for deep soil moisture based on GNSS-R detection data. The deep soil moisture prediction model combines the unsaturated soil infiltration model, Darcy's law, and a soil–water characteristic model. Soil moisture data obtained from humidity sensors in the study area serve as boundary conditions for fitting the soil–water characteristic model parameters. Surface soil moisture data retrieved from GNSS-R signal inversion serve as input variables for the deep soil moisture prediction model, thereby obtaining the monitored deep soil moisture. Section 2.2 describes the construction process of the deep soil moisture prediction model, Section 2.3 describes the data acquisition process, and Section 2.4 describes the validation process of the deep soil moisture prediction model. After validation, the deep soil moisture prediction model can be applied to obtain real-time deep soil moisture data through the real-time surface soil moisture data retrieved from GNSS-R signal inversion, thus facilitating its widespread application. The flowchart of the deep soil moisture prediction method is illustrated in Figure 1 shown below.

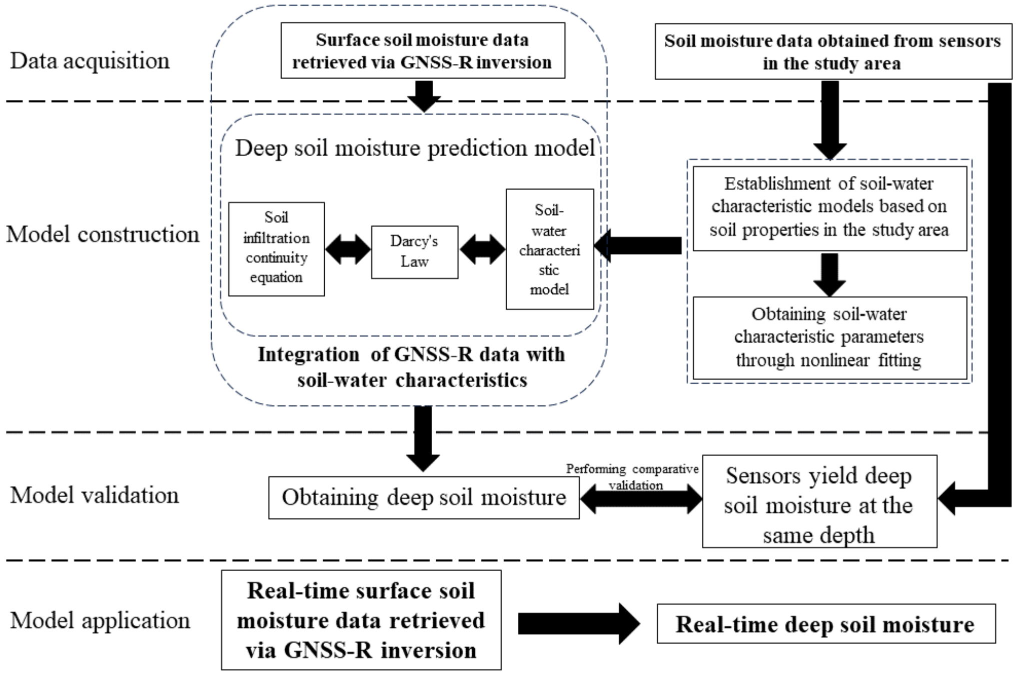

Figure 1. Flowchart of the deep soil moisture prediction method.

2.2. Mathematical Model for Predicting Deep Soil Moisture

2.2.1. Governing Equation of Water Transport in Unsaturated Soil

The Richards equation serves as the governing equation for water movement in unsaturated soil, and it is expressed as a nonlinear partial differential equation. By assuming soil porosity to be uniform and neglecting anisotropy, according to mass conservation, the one-dimensional vertical soil infiltration continuity equation is represented as Equation (1):

$$\frac{\partial\theta}{\partial t} = -\frac{\partial q}{\partial z} \tag{1}$$

where θ is soil moisture, t is the time, q is the vertical infiltration rate perpendicular to the soil surface, and z is the soil depth, with a positive direction oriented vertically downwards (with z = 0 at the soil surface).

Richards introduced Darcy's law into the equation governing unsaturated soil water movement, which can be represented as Equation (2):

$$q = -K\frac{\partial H}{\partial z} = -K\frac{\partial(h-z)}{\partial z} = -K\left(\frac{\partial h}{\partial z} - 1\right) \tag{2}$$

where K is the permeability coefficient, H is the vertical total water potential, and h is the matric suction head.

Furthermore, the expression of the infiltration control equation, known as the Richards equation, can be obtained as shown in Equation (3):

$$\frac{\partial\theta}{\partial t} = \frac{\partial}{\partial z}\left[K\left(\frac{\partial h}{\partial z} - 1\right)\right] \tag{3}$$

To unify the variables, two new variables, C and D, are introduced in Equation (4), representing soil moisture θ and the matric suction head h, respectively:

$$\begin{cases} C(\theta) = \frac{\partial\theta}{\partial h} \\ D(\theta) = \frac{K}{C(\theta)} = \frac{K}{\frac{\partial\theta}{\partial h}} = K\frac{\partial h}{\partial\theta} \end{cases} \tag{4}$$

where C represents the specific water capacity, reflecting the rate at which soil moisture changes with matric suction head and describing the quantitative indicator of the soil's water release capacity, D represents the soil moisture diffusion coefficient, which reflects the soil porosity, the pore size distribution, and its hydraulic conductivity, thereby influencing the soil moisture movement conditions.

By incorporating the specific water capacity, C, and soil moisture diffusion coefficient, D, into the infiltration control equation, as shown in Equation (3) for the Richards equation, we obtain a one-dimensional unsaturated soil water movement control equation with soil moisture θ as the single variable, as shown in Equation (5):

$$\frac{\partial \theta}{\partial t} = \frac{\partial}{\partial z}\left(D(\theta)\frac{\partial \theta}{\partial z}\right) - \frac{\partial K}{\partial z} \tag{5}$$

By defining $V = dK/d\theta = (K(\theta_s) - K(\theta_0))/(\theta_s - \theta_0)$, the one-dimensional unsaturated soil water movement control equation can be transformed into Equation (6):

$$\frac{\partial \theta}{\partial t} = D(\theta)\frac{\partial^2 \theta}{\partial z^2} - V\frac{\partial \theta}{\partial z} \tag{6}$$

2.2.2. Soil–Water Characteristic Model

The soil–water characteristic model is primarily used in soil science to reflect properties such as water retention, moisture movement, and changes in suction. It portrays the functional relationship between soil water energy and soil moisture. From the modern perspective of soil mechanics, the constitutive model of water retention characteristics is one of the constitutive models of unsaturated soil. Therefore, it serves as an important indicator for representing the basic hydraulic properties of soil, and it plays a crucial role in studying soil water retention and movement. The deep soil moisture prediction model proposed in this paper adopts the Van Genuchten model to characterize the soil–water characteristic model, which represents the relationship between soil moisture and suction. The Van Genuchten model is depicted as Equation (7):

$$\begin{cases} h = \frac{1}{\alpha}\left({S_e}^{-\frac{1}{m}} - 1\right)^{\frac{1}{n}} \\ K = K_s \cdot K_r = K_s \cdot {S_e}^{0.5}\left[1 - \left(1 - {S_e}^{1/m}\right)^m\right]^2 \end{cases} \tag{7}$$

where the following applies: S_e is the soil–water saturation, $S_e = (\theta - \theta_r)/(\theta_s - \theta_r)$; θ is the soil moisture; θ_r is the soil residual moisture; θ_s is the soil saturated moisture; h is the soil suction head with the unit in meters (m); α is a fitting parameter related to the soil–air entry value, approximately equal to the reciprocal of the air entry value, with units in meters to the power of negative one (m^{-1}); n is a fitting parameter related to the soil pore size distribution, $n > 1$; m is a fitting parameter associated with the overall symmetry of the soil characteristic curve, $m = 1 - 1/n$ $(0 < m < 1)$; K represents the soil permeability coefficient with units in meters per second (m/s); K_s represents the saturated hydraulic conductivity of the soil with units in meters per second (m/s); and K_r represents the soil relative permeability coefficient, $K_r = K/K_s$.

The parameters α, n, and m in the Van Genuchten model are obtained through the nonlinear fitting of soil moisture at different depths, thereby establishing the soil–water characteristic model.

2.2.3. Model for Predicting Deep Soil Moisture

The present study integrates the equation governing water movement in unsaturated soil with the soil–water characteristic model and further establishes the deep soil moisture prediction model.

In unsaturated infiltration, the relationship between the permeability coefficient, the matric suction head, h, and the variable soil moisture, θ, is a significant factor influencing the nonlinearity of the Richards equation. Therefore, we integrate the soil–water characteristic model with the one-dimensional unsaturated soil water movement control equation, incorporating the Van Genuchten model in terms of specific water capacity, C, and the soil moisture diffusion coefficient, D. This yields Equation (8):

$$\begin{cases} C(\theta) = \frac{\partial h}{\partial \theta} = \frac{1}{n m \alpha} \cdot \left(Se^{-\frac{1}{m}} - 1\right)^{\frac{1}{n}-1} \cdot Se^{-\frac{1}{m}-1} \cdot \frac{1}{\theta_r - \theta_s} \\ D(\theta) = \frac{K}{C(\theta)} = \frac{K}{\frac{\partial \theta}{\partial h}} = K\frac{\partial h}{\partial \theta} = \frac{K}{n m \alpha} \cdot \left(Se^{-\frac{1}{m}} - 1\right)^{\frac{1}{n}-1} \cdot Se^{-\frac{1}{m}-1} \cdot \frac{1}{\theta_r - \theta_s} \end{cases} \tag{8}$$

The method predicts the instantaneous soil moisture of deep soil layers. For instantaneous soil moisture, which remains constant, $\frac{\partial \theta}{\partial t} = 0$, the governing equation for one-dimensional unsaturated soil water transport can be transformed into Equation (9):

$$0 = D(\theta)\frac{\partial^2 \theta}{\partial z^2} - V\frac{\partial \theta}{\partial z} \tag{9}$$

Assuming the diffusion coefficient is constant, $D = D(\theta_0) = \frac{K(\theta_0)}{n m \alpha} \cdot \left(Se^{-\frac{1}{m}} - 1\right)^{\frac{1}{n}-1} \cdot Se^{-\frac{1}{m}-1} \cdot \frac{1}{\theta_r - \theta_s}$, the general solution of the one-dimensional unsaturated soil water transport governing equation is given by Equation (10):

$$\theta = c1 + c2\mathrm{e}^{\frac{V}{D}z} \tag{10}$$

In the equation, $c1$ and $c2$ are undetermined coefficients that can be determined through the boundary conditions at the upper and lower boundaries of the soil layer.

If the surface soil moisture θ_{surface} retrieved from the GNSS signal inversion is known, and the soil moisture θ_0 at a depth of 1 m is obtained through a soil moisture sensor, the undetermined coefficients $c1$ and $c2$ can be determined through Equation (11):

$$\begin{cases} c1 + c2 = \theta_{\text{surface}} \\ c1 + c2 \cdot e^{\frac{V}{D}} = \theta_0 \end{cases} \tag{11}$$

Further simplification leads to Equation (12):

$$\begin{cases} c1 = \frac{\theta_{\text{surface}} \cdot e^{\frac{V}{D}} - \theta_0}{e^{\frac{V}{D}} - 1} \\ c2 = \frac{\theta_{\text{surface}} - \theta_0}{1 - e^{\frac{V}{D}}} \end{cases} \tag{12}$$

Therefore, the particular solution of the one-dimensional unsaturated soil–water movement control equation, representing the relationship between the soil moisture and depth, is given by Equation (13), where the diffusion coefficients D and V are functions of soil–water characteristic parameters α, n, and m.

$$\theta = \frac{\theta_{\text{surface}} \cdot e^{\frac{V(m)}{D(\alpha,m,n)}} - \theta_0}{e^{\frac{V(m)}{D(\alpha,m,n)}} - 1} + \frac{\theta_{\text{surface}} - \theta_0}{1 - e^{\frac{V(m)}{D(\alpha,m,n)}}}\mathrm{e}^{\frac{V(m)}{D(\alpha,m,n)}z} \tag{13}$$

After constructing the deep soil moisture prediction model, this study fits the soil–water characteristic parameters using soil moisture data from different depths. Employing the deep soil moisture prediction model, soil moisture data from two or more different depths obtained from sensors are nonlinearly fitted to obtain the soil–water characteristic parameters α, n, and m, completing the construction of the deep soil moisture prediction model.

After completing the construction of the deep soil moisture prediction model, inputting the surface soil moisture data obtained from GNSS-R signal inversion into the deep soil moisture prediction model allows the relationship between the predicted soil moisture θ and the soil depth z for depths ranging from 0 to 1 m to be determined, as described with Equation (13). This enables the real-time and dynamic monitoring of deep soil moisture over a wide range.

2.3. Obtaining Soil Moisture Data

2.3.1. Soil Moisture Data from Sensors

Using soil moisture sensors to obtain soil moisture at different depths is convenient and direct in field operations, with high data accuracy. The working principles of soil moisture sensors are also diverse. Common soil moisture sensors are based on time-domain reflectometry (TDR), frequency-domain reflectometry (FDR), the standing wave ratio (SWR) method, the capacitance method, the resistance method, or the tensiometer method.

The soil moisture at a depth of 1 m from the surface tends to be relatively stable. Therefore, at a representative location within the monitoring area, the soil moisture at a depth of 1 m was chosen as the lower boundary condition for the deep soil moisture prediction model. Additionally, data from two or more sets of soil moisture at different depths are required from this location to fit the soil–water characteristic model and obtain soil–water characteristic parameters, thus establishing the soil–water characteristic model. Apart from surface soil moisture data obtained through GNSS-R signal inversion, other soil moisture data are acquired using soil moisture sensors. In this study, the soil moisture sensor provided soil moisture θ_0 at a depth of 1 m and several sets of soil moisture θ between 0 and 1 m depth, sourced from the International Soil Moisture Network. The International Soil Moisture Network is a work of international cooperation to establish and maintain a global in situ soil moisture database. This database is an essential means of validating and improving global satellite products and land surface, climate, and hydrological models.

2.3.2. Soil Moisture Data from GNSS-R Inversion

This method requires surface soil moisture data to be obtained from GNSS-R inversion in the monitoring area as input variables for the deep soil moisture prediction model. Due to the high accuracy of surface soil moisture data obtained through GNSS-R signal inversion based on land-based or unmanned aerial vehicle receivers, this study utilized soil moisture sensor measurements sourced from the International Soil Moisture Network to substitute for surface soil moisture obtained from GNSS-R signal inversion.

2.4. Model Verification

2.4.1. Research Area

Due to the real-time prediction method for deep soil moisture relying on GNSS-R detection data, ensuring the accuracy of surface soil moisture retrieved from GNSS-R inversion requires the selection of regions where environmental factors minimally affect GNSS-R signal inversion results. Urban areas are prone to significant interference from various signals and light pollution, which can greatly disrupt GNSS-R signal inversion. Therefore, for our research area, we selected a field in Goodwell, Texas County, Oklahoma, USA (latitude: 36.60° N; longitude: 101.64° W), located far from urban areas, to minimize interference from urban environments. This area is situated in the Great Plains region of the United States, characterized by extensive land distribution with minimal interference factors affecting GNSS-R signals.

2.4.2. Model Verification Process Design

To validate the accuracy of the real-time prediction approach to deep soil moisture combining GNSS-R data and a water movement model in unsaturated soil, we compared the soil moisture data obtained from soil moisture sensors at a specific location in the study area with the soil moisture derived from the proposed method in this study. This comparison aims to determine whether the soil moisture data obtained from the real-time prediction method for deep soil moisture align well with the data obtained from soil moisture sensors. If the agreement is satisfactory, it would demonstrate the feasibility of this real-time prediction approach to deep soil moisture, combining GNSS-R data and a water movement model in unsaturated soil.

The first step involves selecting two random locations, labeled A and B, within the study area as monitoring points. We compared the data obtained from soil moisture sensors at these monitoring points with the soil moisture derived from the novel method proposed in this study, thereby validating the method. Before measuring the soil moisture at the monitoring points, it is essential to establish the soil–water characteristic model and the deep soil moisture prediction model for the study area using soil moisture data collected on a specific day.

We obtained surface soil moisture data, as well as soil moisture data, at depths of 0.1 m, 0.2 m, 0.5 m, and 1 m from the International Soil Moisture Network for a specific day at the monitoring points. Utilizing the surface soil moisture data and data from depths of 0.1 m, 0.2 m, 0.5 m, and 1 m, we performed nonlinear fitting according to Equation (13), thereby obtaining the soil–water characteristic model and the deep soil moisture prediction model for the study area. Subsequently, after obtaining the surface soil moisture data from GNSS-R signal inversion at subsequent time points for the monitoring points, we input these data into the deep soil moisture prediction model to derive the relationship function between soil moisture and depth at the monitoring points. Based on the relationship function between soil moisture and depth at the monitoring points, we obtained the soil moisture at each depth between 0 and 1 m for both monitoring points, A and B, as depicted in Figure 2.

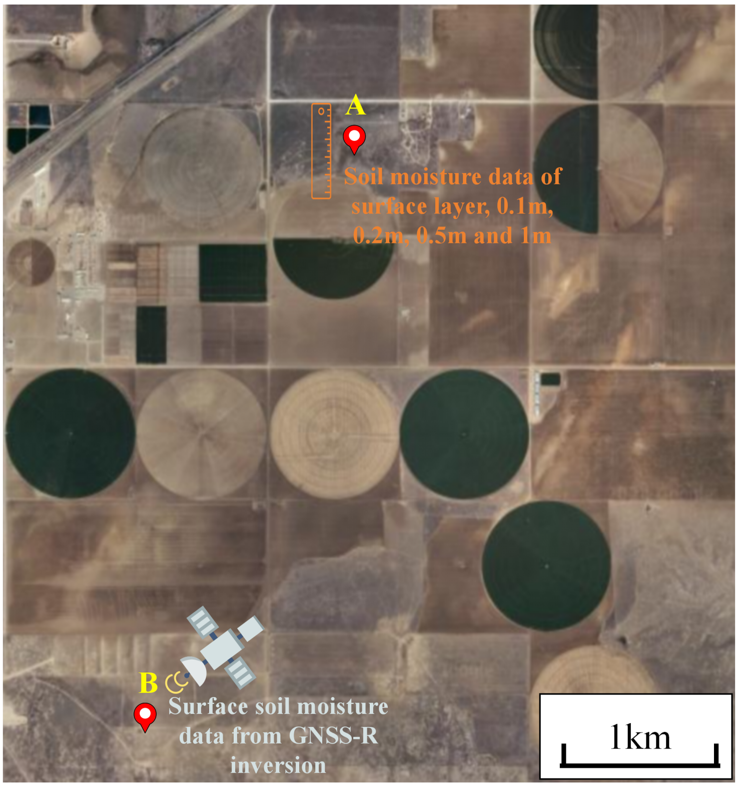

Figure 2. Position relationship diagram between monitoring point **A** and monitoring point **B**.

Afterwards, soil moisture sensors could be utilized to measure the soil moisture at the surface and at depths of 0.1 m, 0.2 m, 0.5 m, and 1 m at the monitoring points. The measured results could then be compared with the results obtained from the real-time prediction method for deep soil moisture, which integrates GNSS-R detection data and soil–water characteristics. This comparison serves to validate the feasibility of the real-time prediction approach to deep soil moisture combining GNSS-R data and a water movement model in unsaturated soil.

2.4.3. Model Evaluation Index

In this paper, the data obtained from the real-time prediction approach to deep soil moisture combining GNSS-R data and a water movement model in unsaturated soil are considered predicted values, while the data obtained from soil moisture sensors are regarded as true values. Statistical indicators such as relative error (δ) and mean square error (MSE) are employed to measure the deviation of predicted values from true values. Additionally, the coefficient of determination (R^2) is used to assess the degree of agreement between predicted values and true values, thereby determining whether the prediction model can accurately forecast deep soil moisture. This process aims to validate the feasibility of the real-time prediction approach to deep soil moisture combining GNSS-R data and water movement model in unsaturated soil.

We represent the true values using TR (m^3/m^3) and the predicted values using PV (m^3/m^3). The absolute error (Δ) is defined as the difference between the predicted value, PV, and the true value, TR, as shown in Equation (14).

$$\Delta = PV - TR \tag{14}$$

The relative error (δ) is defined as the absolute error (Δ) divided by the true value (TR) multiplied by 100% to obtain a percentage representation, as shown in Equation (15).

$$\delta = \frac{\Delta}{TR} \times 100 \tag{15}$$

The mean square error (MSE) is defined as the expected value of the square of the difference between the predicted value, PV, and the true value, TR, as shown in Equation (16). A mean square error (MSE) closer to 0 indicates the better predictive performance of the prediction model.

$$MSE = \frac{1}{m} \sum_{i=1}^{m} (PV_i - TR_i)^2 \tag{16}$$

The coefficient of determination (R^2), also known as the goodness of fit, is commonly used in predictive models to assess the degree of agreement between predicted values and true values. A coefficient of determination (R^2) closer to 1 indicates the better predictive performance of the model. The coefficient of determination (R^2) is expressed in Equation (17).

$$R^2 = 1 - \frac{\sum_{i=1}^{m} (PV_i - TR_i)^2}{\sum_{i=1}^{m} (\overline{TR_i} - TR_i)^2} \tag{17}$$

in which $\overline{TR_i}$ represents the mean value of the true values.

3. Results

Firstly, soil moisture data at the surface and depths of 0.1 m, 0.2 m, 0.5 m, and 1 m at monitoring points A and B were obtained from the International Soil Moisture Network for 20 October, 25 October, 30 October, 4 November, 9 November, 14 November, and 19 November 2023. The soil moisture data from 25 October, 30 October, 4 November, 9 November, 14 November, and 19 November 2023 at monitoring points A and B were primarily used to compare with the results obtained from the real-time prediction approach for deep soil moisture proposed in this paper. The soil moisture data from 20 October 2023 at monitoring points A and B were mainly used to establish the soil–water characteristic model and the deep soil moisture prediction model for the study area.

Next, using the soil moisture data from monitoring points A and B at the surface and depths of 0.1 m, 0.2 m, 0.5 m, and 1 m on 20 October 2023, we performed the nonlinear fitting of Equation (13) to establish the soil–water characteristic model and the deep soil moisture prediction model for the study area. Subsequently, utilizing the surface soil moisture data from monitoring points A and B on 25 October, 30 October, 4 November, 9 November, 14 November, and 19 November 2023, we obtained the predicted values of soil moisture at depths from 0 to 1 m using the deep soil moisture prediction model.

Finally, the predicted values and true values of soil moisture at the surface and depths of 0.1 m, 0.2 m, 0.5 m, and 1 m for monitoring points A and B on the six dates were compared. The results are shown in Figures 3 and 4. From the figures, it can be qualitatively observed that the predicted values of soil moisture at the monitoring points correspond well with the true values.

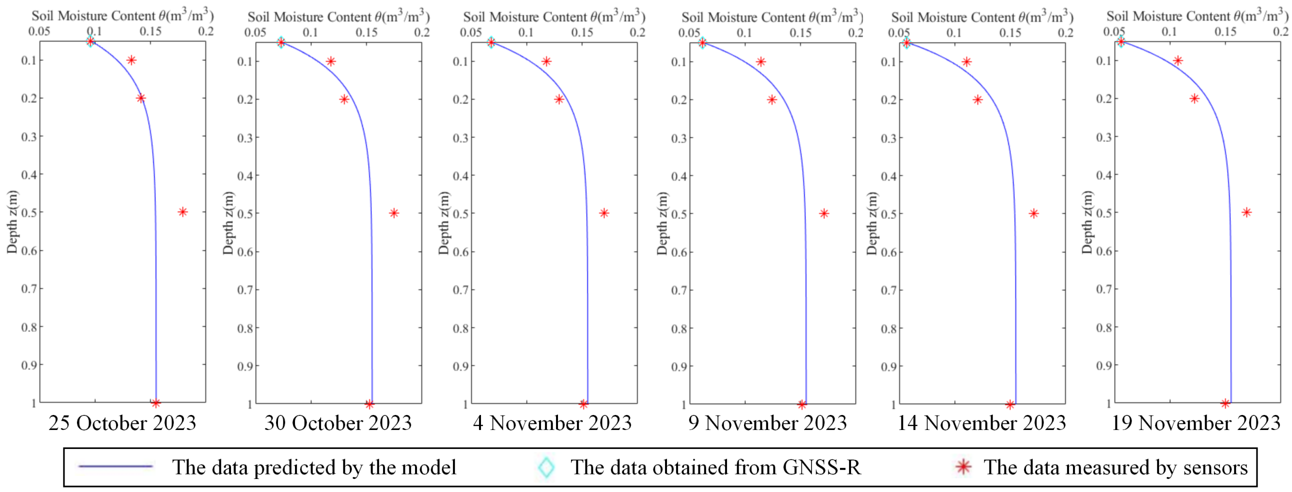

Figure 3. Comparison between predicted and true soil moisture values at monitoring point A over six days.

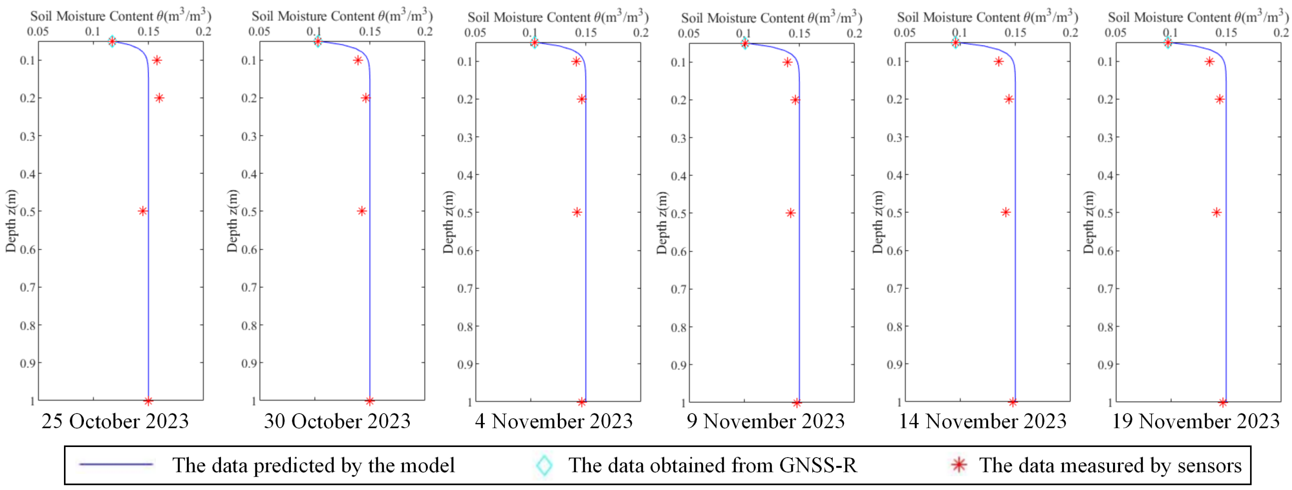

Figure 4. Comparison between predicted and true soil moisture values at monitoring point B over six days.

3.1. Assessment of Predicted Values

3.1.1. Relative Error of the Predicted Values

Subsequently, the relative error (δ) between the predicted and true soil moisture values at different depths for monitoring points A and B over the six days was utilized to quantitatively evaluate the accuracy of the model predictions, as depicted in Figures 5 and 6. On 25 October 2023, the relative error (δ) of the predicted soil moisture values at different depths for monitoring point A ranged from −13.97% to 0.71%, while for monitoring point B, it ranged from −6.25% to 3.45%. Similarly, on 30 October 2023, the relative error (δ) for monitoring point A varied from −12.00% to 5.38%, and for monitoring point B, it ranged from 2.74% to 6.47%. On 4 November 2023, the relative error (δ) for monitoring point A ranged from −12.71% to 5.43%, while for monitoring point B, it ranged from −2.74% to 5.63%. On 9 November 2023, the relative error (δ) for monitoring point A ranged from −13.16% to 8.87%, and for monitoring point B, it ranged from 1.35% to 6.47%. On 14 November 2023, the relative error (δ) for monitoring point A varied from −13.51% to 10.74%, and for monitoring point B, it ranged from 1.35% to 9.63%. Finally, on 19 November 2023, the relative error (δ) for monitoring point A ranged from −10.28% to 9.84%, while for monitoring point B, it ranged from 2.04% to 9.63%. The relative errors (δ) of soil moisture predictions relative to true values at different depths for monitoring points A and B over the six days were all within a small range, indicating minimal deviation between predicted and true soil moisture values. Therefore, this validates the feasibility of the real-time prediction approach to deep soil moisture combining GNSS-R data and a water movement model in unsaturated soil.

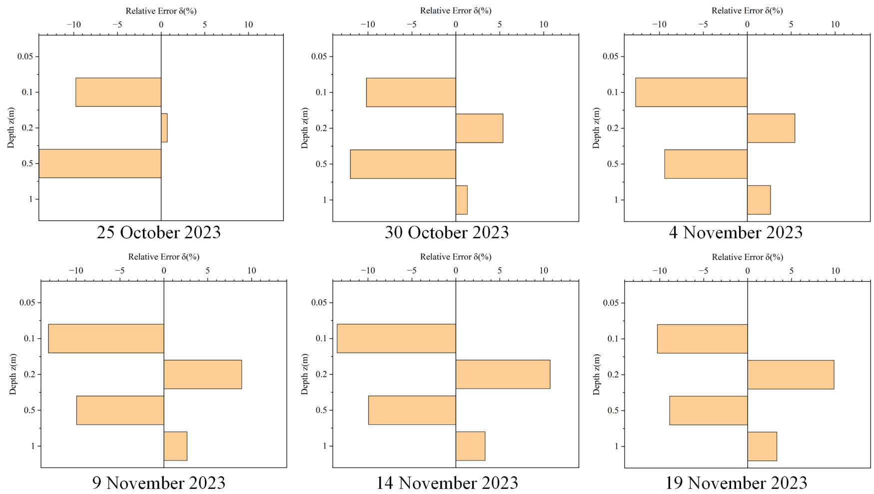

Figure 5. The relative errors of soil moisture predictions at different depths for monitoring point A over six days.

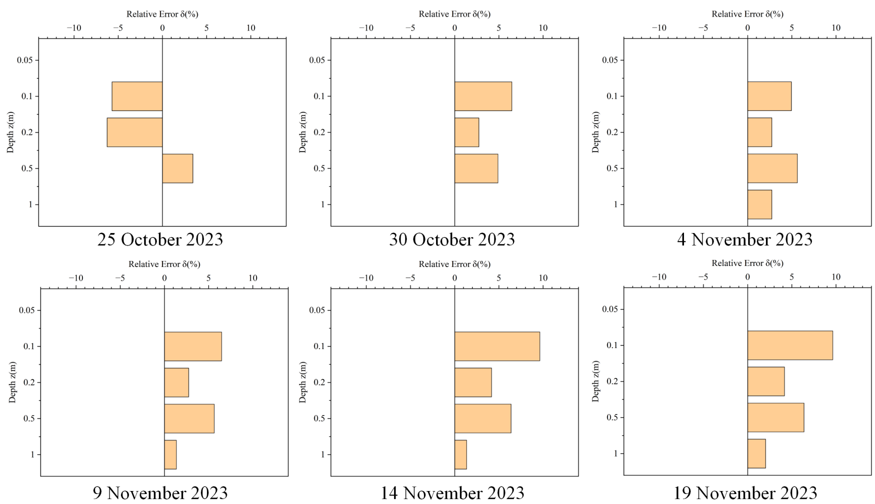

Figure 6. The relative errors of soil moisture predictions at different depths for monitoring point B over six days.

3.1.2. MSE and R^2 of the Predicted Values

Based on the mean square error (MSE) and the coefficient of determination (R^2) relative to the true values of soil moisture predictions over the six days, a more in-depth quantitative analysis of the model's prediction accuracy could be conducted.

According to computations, the mean square error (MSE) of soil moisture predictions for monitoring point A on 25 October 2023 was 1.59×10^{-4}, while for monitoring point B, it was 4.12×10^{-5}. On 30 October 2023, the MSE for monitoring point A was 1.28×10^{-4}, and for monitoring point B, it was 2.92×10^{-5}. For 4 November 2023, the MSE for monitoring point A was 1.09×10^{-4}, and for monitoring point B, it was 2.90×10^{-5}. On 9 November 2023, the MSE for monitoring point A was 1.30×10^{-4}, and for monitoring point B, it was 3.30×10^{-5}. For 14 November 2023, the MSE for monitoring point A was 1.42×10^{-4}, and for monitoring point B, it was 5.80×10^{-5}. Finally, on 19 November 2023, the MSE for monitoring point A was 1.03×10^{-4}, and for monitoring point B, it was 5.90×10^{-5}, as shown in Figures 7 and 8. It is evident that the prediction accuracy from the surface to the deep soil moisture prediction models shows a high degree of fit with the true values. Therefore, it validates the feasibility of the real-time prediction approach to deep soil moisture combining GNSS-R data and a water movement model in unsaturated soil.

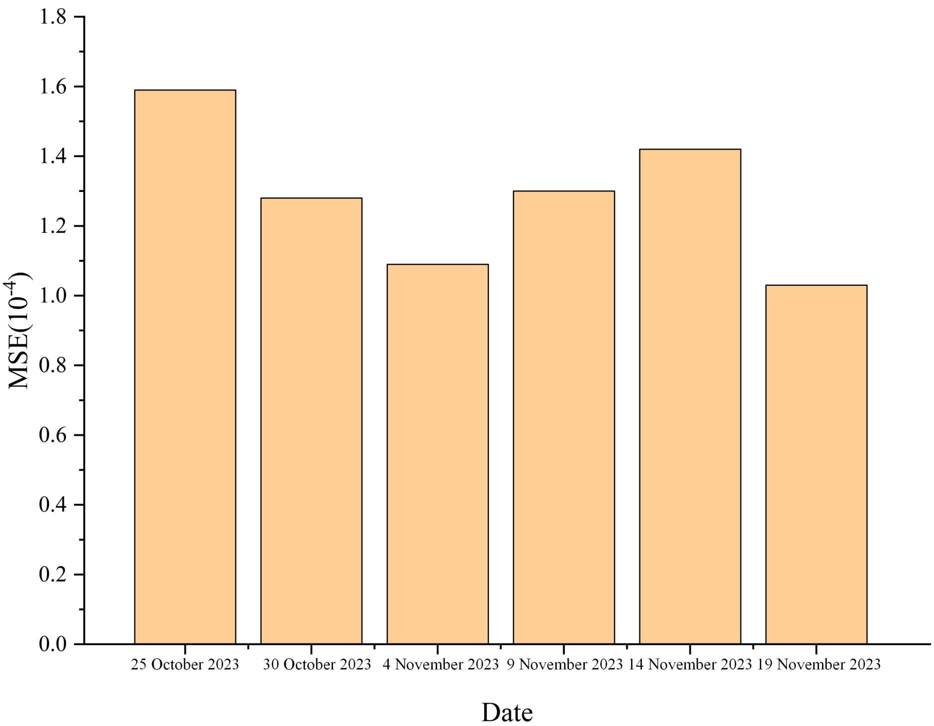

Figure 7. The mean square error (MSE) of monitoring point A over six days.

Through calculations, it was determined that the coefficient of determination R^2 for the soil moisture predictions at monitoring point A on 25 October 2023 was 78.68%, while at monitoring point B, it was 82.80%. On 30 October 2023, the coefficient of determination R^2 for soil moisture predictions at monitoring point A was 89.27%, and at monitoring point B, it was 89.88%. By 4 November 2023, the coefficient of determination R^2 for soil moisture predictions at monitoring point A increased to 90.89%, whereas at monitoring point B, it decreased slightly to 88.71%. On 9 November 2023, the coefficient of determination R^2 for soil moisture predictions at monitoring point A was 90.54%, and at monitoring point B, it was 89.08%. By 14 November 2023, the coefficient of determination R^2 for soil moisture predictions at monitoring point A was 90.60%, and at monitoring point B, it was 83.73%. Finally, on 19 November 2023, the coefficient of determination R^2 for soil moisture predictions at monitoring point A was 93.19%, while at monitoring point B, it was 82.45%, as illustrated in Figures 9 and 10. It is evident that the predictive models for soil moisture content from the surface to deep layers exhibit a high degree of conformity between predicted and actual values. Therefore, the feasibility of the real-time prediction approach to deep soil moisture content, which integrates GNSS-R detection data and soil moisture characteristics, can be validated.

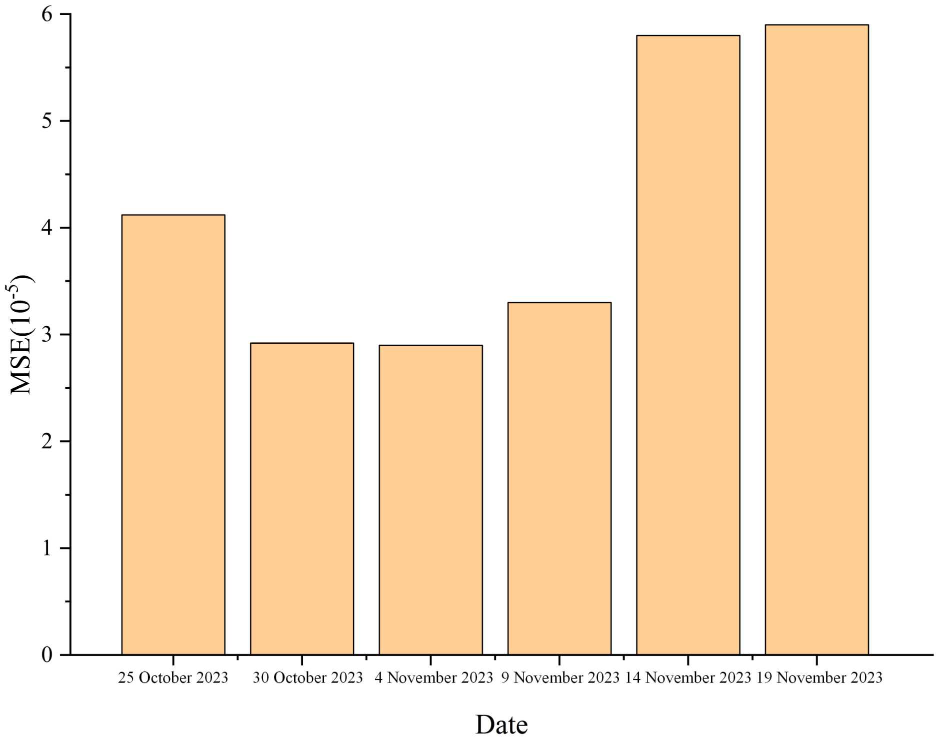

Figure 8. The mean square error (MSE) of monitoring point B over six days.

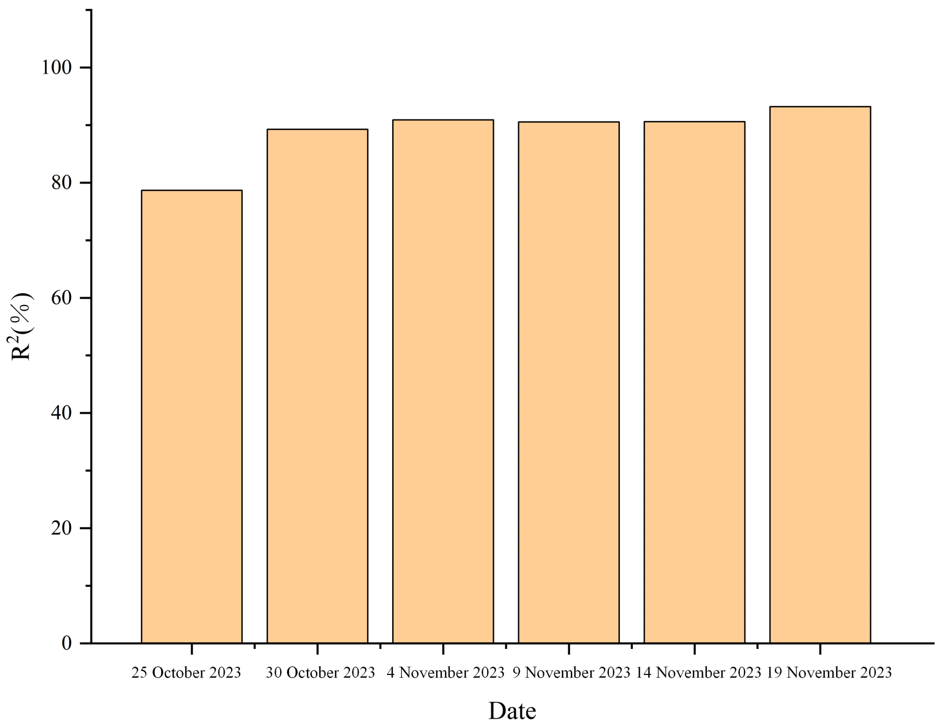

Figure 9. The coefficient of determination (R^2) for monitoring point A's soil moisture prediction over six days.

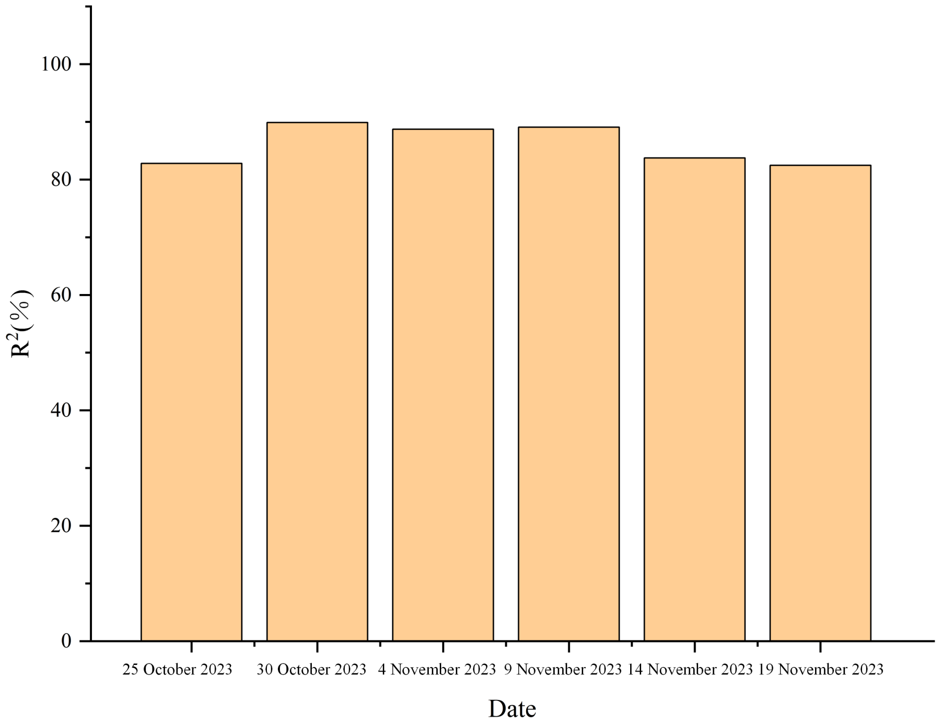

Figure 10. The coefficient of determination (R^2) for monitoring point B's soil moisture prediction over six days.

When combining the mean square errors (MSEs) and coefficients of determination (R^2) relative to the true values for soil moisture predictions at monitoring points A and B at depths from the surface of 0.1 m, 0.2 m, 0.5 m, and 1 m on 25 October, 30 October, 4 November, 9 November, 14 November, and 19 November 2023, it is evident that the deep soil moisture prediction model achieves a high degree of fit between predicted and actual values. Thus, it validates the feasibility of the real-time prediction approach to deep soil moisture combining GNSS-R data and water movement model in unsaturated soil.

3.2. Effects of Soil–Water Characteristic Model on Predicted Values

Using the real-time prediction approach to deep soil moisture combining GNSS-R data and a water movement model in unsaturated soil, soil moisture predictions for monitoring points A and B on 25 October 2023 were obtained, revealing significant discrepancies in the predicted values, as shown in Figure 11. The deep soil moisture prediction model used for monitoring both points, A and B, is consistent, with the only variable being the soil–water characteristic parameters α, n, and m in the deep soil moisture prediction model. However, these parameters, α, n, and m, are related to the soil properties at monitoring points A and B. Therefore, a comparison of the soil–water characteristic models between monitoring points A and B was warranted.

Figure 12 illustrates the permeability coefficient characteristic curves of monitoring points A and B, while Figure 13 depicts the matric suction head characteristic curves of monitoring points A and B. It can be observed that the infiltration coefficient characteristic curves of monitoring points A and B are relatively similar, whereas the matric suction head characteristic curves of monitoring points A and B exhibit significant differences. This discrepancy contributes to the considerable disparity in the predicted soil moisture between monitoring points A and B.

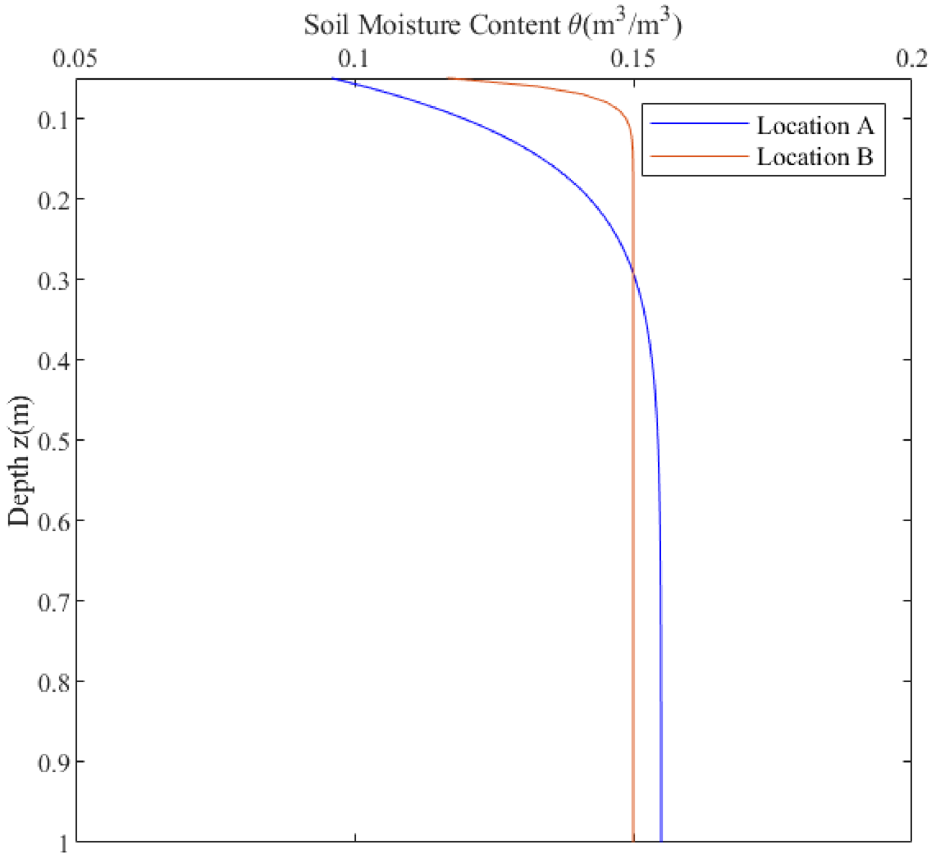

Figure 11. The comparison of predicted values between monitoring points A and B.

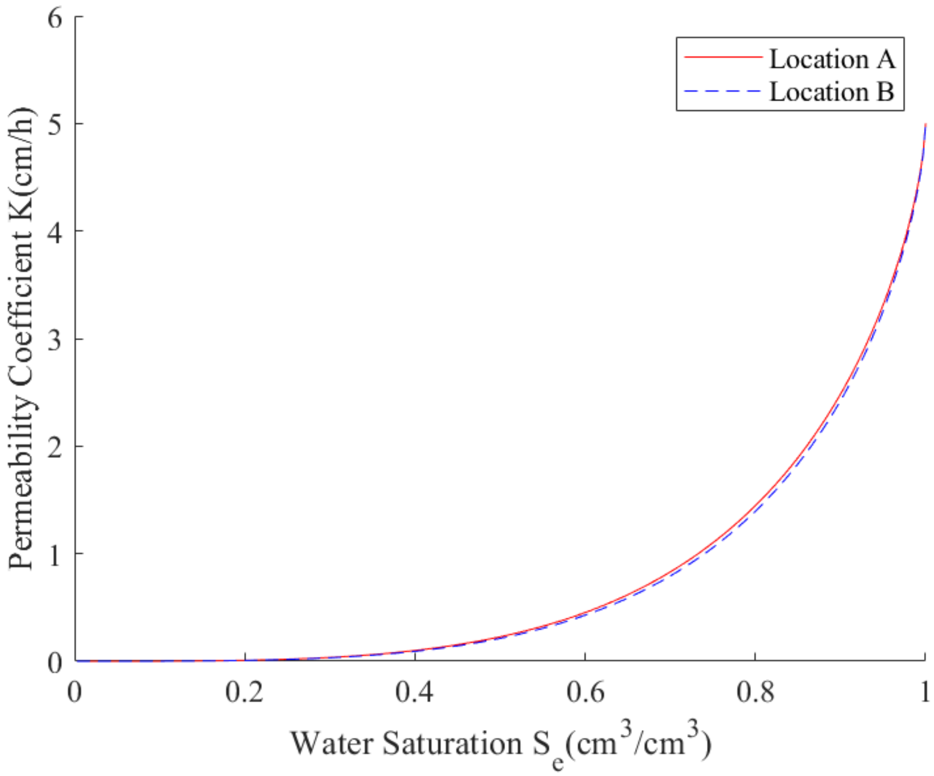

Figure 12. The comparison of the permeability coefficient characteristic curves between monitoring points A and B.

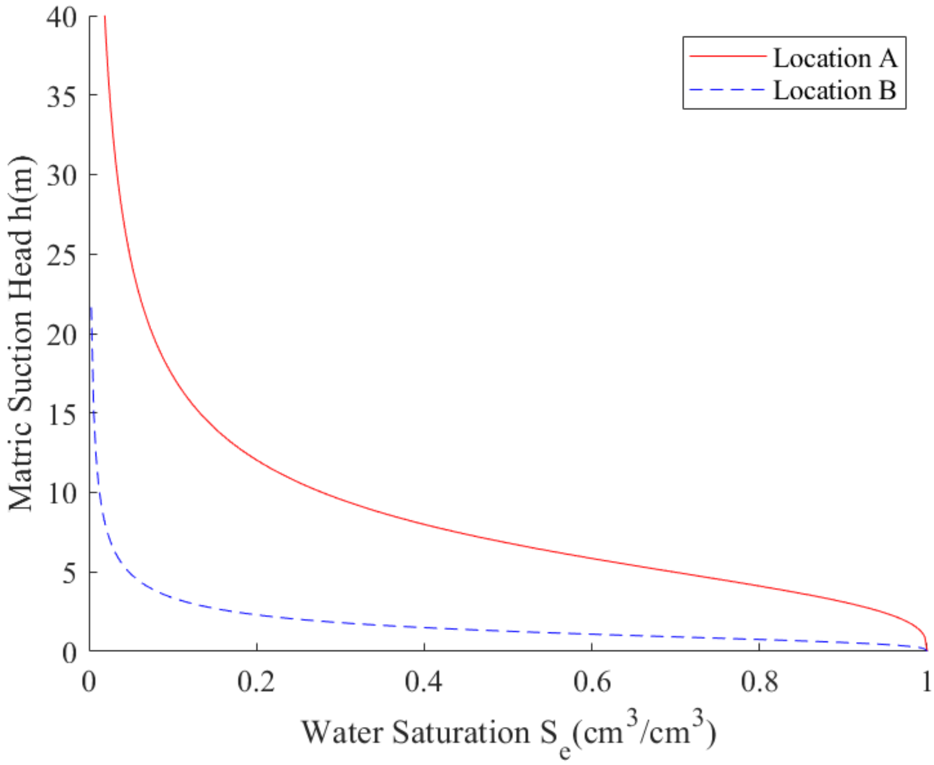

Figure 13. The comparison of matric suction head characteristic curves between monitoring points A and B.

3.3. Effects of Model Lower Boundary Depth on Predicted Values

The real-time prediction approach to deep soil moisture combining GNSS-R data and a water movement model in unsaturated soil proposed in this paper sets the depth of the lower boundary of the moisture movement control equation in unsaturated soil to 1 m. To investigate the influence of the lower boundary depth setting on soil moisture prediction, this paper sets the lower boundary depth to 1 m, 10 m, 20 m, 30 m, 40 m, and 50 m, obtaining the corresponding predicted values for monitoring point A on 25 October 2023 and comparing them, as shown in Figure 14.

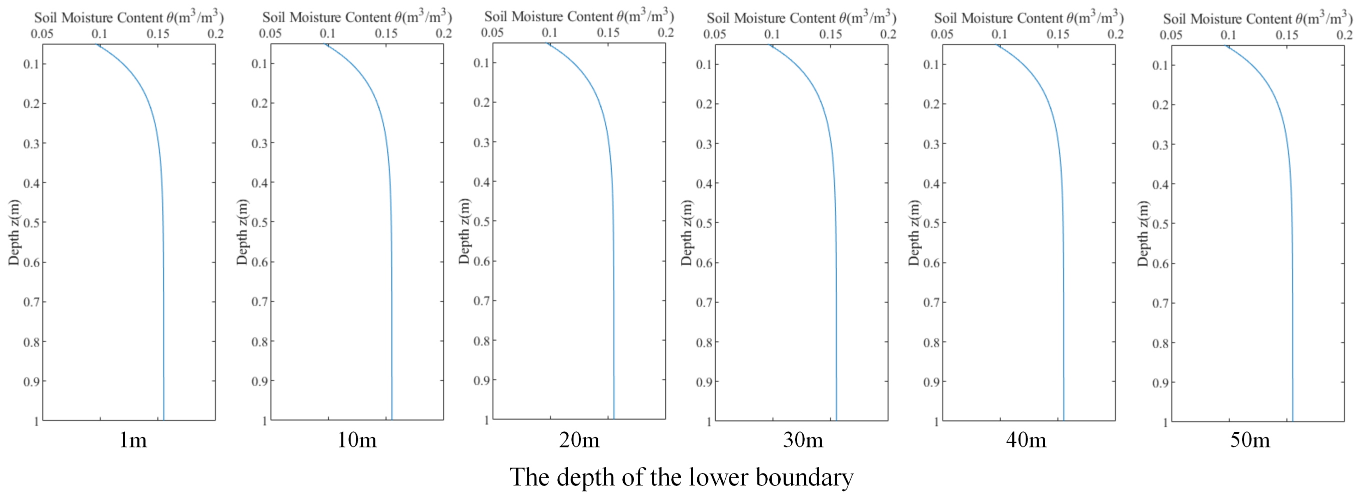

Figure 14. The comparison of the permeability coefficient characteristic curves between monitoring point A and monitoring point B.

From the graph, it can be observed that the lower boundary depth of the unsaturated soil moisture movement control equation has no effect on soil moisture prediction values when it exceeds 1 m. Therefore, choosing 1 m as the lower boundary depth of the unsaturated soil moisture movement control equation is reasonable.

4. Discussion

Due to the close correlation between soil moisture and variables such as soil properties and climatic conditions, the deep soil moisture prediction model proposed in this paper incorporates variables such as soil properties and climatic conditions during the construction process, aiming to achieve applicability under different soil properties and climatic conditions. As our model integrates the soil–water characteristic model, the deep soil moisture prediction model we obtained is parameterized. Through the initial data fitting process, the parameters in the model are solved, reflecting the characteristics of soil types. Since the soil composition in many regions within the depth range of 0–1 m is relatively homogeneous, resembling a homogeneous porous medium, our model is applicable in regions where the soil composition is uniform.

In cases of heterogeneous soil, it is possible to conduct stratified research on the soil in the study area. By combining the corresponding soil–water characteristic parameters of each soil layer, our model can be applied to conduct research effectively. Due to the close correlation between surface soil moisture data and climatic conditions, incorporating GNSS-R-retrieved surface soil moisture data into the process of predicting deep soil moisture through modeling implies that the model takes climate condition variables into consideration. In summary, the real-time prediction approach to deep soil moisture combining GNSS-R data and a water movement model in unsaturated soil proposed in this paper exhibits strong applicability and holds potential for future deployment in various regions. However, further optimization is necessary to enhance the method's universality.

5. Conclusions

The real-time monitoring of deep soil moisture has significant implications for controlling the quality of compacted soil construction, geological disaster monitoring and forecasting, the precise management of agricultural production, and other areas. However, traditional methods of soil moisture monitoring suffer from inefficiency and high costs when applied to large-scale areas. Additionally, methods that rely on GNSS-R signal inversion to obtain soil moisture data are limited due to their shallow monitoring depth. To address the limitations of current soil moisture monitoring methods, particularly their inability to dynamically monitor deep soil moisture over large areas in real time, this study innovatively proposed a real-time prediction approach to deep soil moisture combining GNSS-R data and a water movement model in unsaturated soil. This approach utilizes surface soil moisture data obtained through GNSS-R signal inversion and integrates it with soil–water characteristics and soil moisture data at a depth of 1 m. By employing a deep soil moisture prediction model, it is possible to obtain predicted soil moisture values for depths ranging from 0 to 1 m, enabling the large-scale, real-time monitoring of deep soil moisture. The proposed method was validated using data provided by the International Soil Moisture Network, focusing on a field in Goodwell, Texas County, OK, USA, as the study area.

By calculating the relative error δ of the predicted soil moisture values relative to the true values at monitoring points A and B in the study area at the surface and depths of 0.1 m, 0.2 m, 0.5 m, and 1 m on six days (25 October, 30 October, 4 November, 9 November, 14 November, and 19 November 2023), it was found that the relative error δ remained within a relatively low range. The relative error δ at monitoring point A was controlled within $\pm$14%, while at monitoring point B, it was controlled within $\pm$10%. Therefore, it is evident that the deep soil moisture prediction model fits the true values quite well. Furthermore, by computing the mean square error (MSE) and coefficient of determination (R^2) of the soil moisture predictions relative to the true values at monitoring points A and B in the study area at the surface and depths of 0.1 m, 0.2 m, 0.5 m, and 1 m on the same six days, it was observed that the MSE at monitoring point A ranged from 1.03×10^{-4} to 1.59×10^{-4}, and at monitoring point B, it ranged from 2.90×10^{-5} to 5.90×10^{-5}, indicating a relatively low overall control level. The R^2 at monitoring point A ranged from 78.68% to 93.19%, while at monitoring point B, it ranged from 82.45% to 89.88%, indicating a relatively high overall control level. Therefore, it can be concluded that the deep soil moisture prediction model achieves a high level of fitting with the true values. Consequently, the soil moisture data predicted using this method align well with actual soil moisture data, validating the feasibility of the real-time prediction approach to deep soil moisture combining GNSS-R data and a water movement model in unsaturated soil. The soil–water characteristic model influences soil moisture prediction values, rendering the method applicable across different geographic features. Moreover, the depth of the lower boundary in the unsaturated soil moisture transport control equation does not affect soil moisture prediction values when it exceeds 1 m, justifying the selection of 1 m as a reasonable depth for the lower boundary in the unsaturated soil moisture transport control equation.

The real-time prediction approach to deep soil moisture combining GNSS-R data and a water movement model in unsaturated soil achieves the real-time and dynamic monitoring of deep soil moisture over a wide range, which can play a significant role in various fields, such as agricultural production, geological disaster management, engineering construction, and heritage preservation.

Author Contributions: Conceptualization, H.S.; methodology, H.S. and X.L.; software, C.Y.; validation, Y.S., W.B. and C.Y.; formal analysis, W.L.; investigation, X.L.; resources, Y.S., W.B. and W.L.; data curation, W.B. and C.Y.; writing—original draft preparation, X.L.; writing—review and editing, H.S.; supervision, Y.S., W.B. and W.L.; project administration, Y.S., H.S. and W.L. All authors have read and agreed to the published version of the manuscript.

Funding: This work is supported by the Youth Cross Team Scientific Research Project of the Chinese Academy of Sciences (JCTD-2021-10) and in part by National Natural Science Foundation of China 42074042 and 42104032.

Data Availability Statement: The original contributions presented in the study are included in the article, further inquiries can be directed to the corresponding author.

Conflicts of Interest: The authors declare no conflicts of interest.

References

1. Craig, R.F. *Craig's Soil Mechanics*; CRC Press: Boca Raton, FL, USA, 2004.
2. Das, B.M. *Principles of Geotechnical Engineering*; Cengage Learning: Boston, MA, USA, 2021.
3. Gardner, W. The capillary potential and its relation to soilmoisture constants. *Soil Sci.* **1920**, *10*, 357–360. [CrossRef]
4. Gardner, W.; Widtsoe, J.A. The movement of soil moisture. *Soil Sci.* **1921**, *11*, 215–232. [CrossRef]
5. Haines, W.B. The volume-changes associated with variations of water content in soil. *J. Agric. Sci.* **1923**, *13*, 296–310. [CrossRef]
6. Pham, H.Q.; Fredlund, D.G.; Barbour, S.L. A study of hysteresis models for soil-water characteristic curves. *Can. Geotech. J.* **2005**, *42*, 1548–1568. [CrossRef]
7. Richards, L.A. Capillary conduction of liquids through porous mediums. *Physics* **1931**, *1*, 318–333. [CrossRef]
8. Brooks, R.H. *Hydraulic Properties of Porous Media*; Colorado State University: Fort Collins, CO, USA, 1965.
9. Van Genuchten, M.T. A closed-form equation for predicting the hydraulic conductivity of unsaturated soils. *Soil Sci. Soc. Am. J.* **1980**, *44*, 892–898. [CrossRef]
10. Baver, L.D. *Soil Physics*; John Wiley and Sons, Inc.: New York, NY, USA, 1956; Volume 81.
11. Fang, H.Y.; Daniels, J.L. *Introductory Geotechnical Engineering: An Environmental Perspective*; CRC Press: Boca Raton, FL, USA, 2017.
12. Kaplan, E.D.; Hegarty, C. *Understanding GPS/GNSS: Principles and Applications*; Artech House: Boston, MA, USA, 2017.
13. Wigneron, J.P.; Jackson, T.J.; O'Neill, P.; De Lannoy, G.; de Rosnay, P.; Walker, J.P.; Ferrazzoli, P.; Mironov, V.; Bircher, S.; Grant, J.P. Modelling the passive microwave signature from land surfaces: A review of recent results and application to the L-band SMOS and SMAP soil moisture retrieval algorithms. *Remote Sens. Environ.* **2017**, *192*, 238–262. [CrossRef]

14. Masters, D.; Axelrad, P.; Katzberg, S. Initial results of land-reflected GPS bistatic radar measurements in SMEX02. *Remote Sens. Environ.* **2004**, *92*, 507–520. [CrossRef]
15. Egido, A.; Ruffini, G.; Caparrini, M.; Martin, C.; Farres, E.; Banque, X. Soil moisture monitorization using GNSS reflected signals. *arXiv* **2008**, arXiv:0805.1881.
16. Kebiao, M.; Mengyang, Z.; Jianming, W.; Huajun, T.; Qingbo, Z. The study of soil moisture retrieval algorithm from gnss-r. In Proceedings of the 2008 International Workshop on Education Technology and Training & 2008 International Workshop on Geoscience and Remote Sensing, Shanghai, China, 21–22 December 2008; Volume 1, pp. 438–442.
17. Sreedeep, S.; Reshma, A.C.; Singh, D.N. Measuring soil electrical resistivity using a resistivity box and a resistivity probe. *Geotech. Test. J.* **2004**, *27*, 411–415. [CrossRef]
18. Whalley, W.R.; Dean, T.J.; Izzard, P. Evaluation of the capacitance technique as a method for dynamically measuring soil water content. *J. Agric. Eng. Res.* **1992**, *52*, 147–155. [CrossRef]
19. Schwartz, B.F.; Schreiber, M.E.; Yan, T. Quantifying field-scale soil moisture using electrical resistivity imaging. *J. Hydrol.* **2008**, *362*, 234–246. [CrossRef]
20. Robinson, D.A.; Campbell, C.S.; Hopmans, J.W.; Hornbuckle, B.K.; Jones, S.B.; Knight, R.; Ogden, F.; Selker, J.; Wendroth, O. Soil moisture measurement for ecological and hydrological watershed-scale observatories: A review. *Vadose Zone J.* **2008**, *7*, 358–389. [CrossRef]
21. ASTM Committee D-18 on Soil and Rock. *Standard Test Methods for Laboratory Determination of Water (Moisture) Content of Soil and Rock by Mass*; ASTM: West Conshohocken, PA, USA, 2005.
22. Hillel, D. *Introduction to Soil Physics*; Academic Press: Cambridge, MA, USA, 2013.
23. Zazueta, F.S.; Xin, J. Soil moisture sensors. *Soil Sci.* **1994**, *73*, 391–401.
24. Selig, E.T.; Mansukhani, S. Relationship of soil moisture to the dielectric property. *J. Geotech. Eng. Div.* **1975**, *101*, 755–770. [CrossRef]
25. Topp, G.C.; Davis, J.L.; Annan, A.P. Electromagnetic determination of soil water content using TDR: I. Applications to wetting fronts and steep gradients. *Soil Sci. Soc. Am. J.* **1982**, *46*, 672–678. [CrossRef]
26. Campbell, J.E. Dielectric properties and influence of conductivity in soils at one to fifty megahertz. *Soil Sci. Soc. Am. J.* **1990**, *54*, 332–341. [CrossRef]
27. Arulanandan, K. Dielectric method for prediction of porosity of saturated soil. *J. Geotech. Eng.* **1991**, *117*, 319–330. [CrossRef]
28. Jacobsen, O.H.; Schjønning, P. A laboratory calibration of time domain reflectometry for soil water measurement including effects of bulk density and texture. *J. Hydrol.* **1993**, *151*, 147–157. [CrossRef]
29. Robinson, M.; Dean, T.J. Measurement of near surface soil water content using a capacitance probe. *Hydrol. Processes* **1993**, *7*, 77–86. [CrossRef]
30. Gaskin, G.J.; Miller, J.D. Measurement of soil water content using a simplified impedance measuring technique. *J. Agric. Eng. Res.* **1996**, *63*, 153–159. [CrossRef]
31. Gardner, C.; Dean, T.J.; Cooper, J.D. Soil water content measurement with a high-frequency capacitance sensor. *J. Agric. Eng. Res.* **1998**, *71*, 395–403. [CrossRef]
32. Rinaldi, V.A.; Francisca, F.M. Impedance analysis of soil dielectric dispersion (1 MHz–1 GHz). *J. Geotech. Geoenvironmental Eng.* **1999**, *125*, 111–121. [CrossRef]
33. Baumhardt, R.L.; Lascano, R.J.; Evett, S.R. Soil material, temperature, and salinity effects on calibration of multisensor capacitance probes. *Soil Sci. Soc. Am. J.* **2000**, *64*, 1940–1946. [CrossRef]
34. Hilhorst, M.A. A pore water conductivity sensor. *Soil Sci. Soc. Am. J.* **2000**, *64*, 1922–1925. [CrossRef]
35. Kelleners, T.J.; Soppe, R.; Ayars, J.E.; Skaggs, T.H. Calibration of capacitance probe sensors in a saline silty clay soil. *Soil Sci. Soc. Am. J.* **2004**, *68*, 770–778. [CrossRef]
36. Rohini, K.; Singh, D.N. Methodology for determination of electrical properties of soils. *J. Test. Eval.* **2004**, *32*, 62–68. [CrossRef]
37. Rao, B.H.; Singh, D.N. Moisture content determination by TDR and capacitance techniques: A comparative study. *Int. J. Earth Sci. Eng* **2011**, *4*, 132–137.
38. Mittelbach, H.; Lehner, I.; Seneviratne, S.I. Comparison of four soil moisture sensor types under field conditions in Switzerland. *J. Hydrol.* **2012**, *430*, 39–49. [CrossRef]
39. Bowers, S.A. *Reflection of Radiant Energy from Soils*; Kansas State University: Manhattan, KS, USA, 1971.
40. Li, Z.L.; Leng, P.; Zhou, C.; Chen, K.S.; Zhou, F.C.; Shang, G.F. Soil moisture retrieval from remote sensing measurements: Current knowledge and directions for the future. *Earth-Sci. Rev.* **2021**, *218*, 103673. [CrossRef]
41. Edokossi, K.; Calabia, A.; Jin, S.; Molina, I. GNSS-reflectometry and remote sensing of soil moisture: A review of measurement techniques, methods, and applications. *Remote Sens.* **2020**, *12*, 614. [CrossRef]
42. Shen, X.; Walker, J.P.; Ye, N.; Wu, X.; Boopathi, N.; Yeo, I.Y.; Zhang, L.; Zhu, L. Soil moisture retrieval depth of P-and L-band radiometry: Predictions and observations. *IEEE Trans. Geosci. Remote Sens.* **2020**, *59*, 6814–6822. [CrossRef]
43. Shi, Y.; Ren, C.; Yan, Z.; Lai, J. High spatial-temporal resolution estimation of ground-based global navigation satellite system interferometric reflectometry (GNSS-IR) soil moisture using the genetic algorithm back propagation (GA-BP) neural network. *ISPRS Int. J. Geo-Inf.* **2021**, *10*, 623. [CrossRef]

44. Liang, Y.j.; Ren, C.; Wang, H.Y.; Huang, Y.B.; Zheng, Z.T. Research on soil moisture inversion method based on GA-BP neural network model. *Int. J. Remote Sens.* **2019**, *40*, 2087–2103. [CrossRef]
45. Shi, Y.; Ren, C.; Yan, Z.; Lai, J. Improving soil moisture retrieval from GNSS-interferometric reflectometry: Parameters optimization and data fusion via neural network. *Int. J. Remote Sens.* **2021**, *42*, 9085–9108. [CrossRef]